

海水融解水による夏季北極海の海洋 CO₂ 吸収の抑制

小杉 如央¹、笹野 大輔¹、石井 雅男¹、西野 茂人²、内田 裕²、吉川 久幸³

¹ 気象研、² JAMSTEC、³ 北大環境科学院

Sea ice melt water hampers air-sea CO₂ flux in the Arctic Ocean

Naohiro Kosugi¹, Daisuke Sasano¹, Masao Ishii¹, Shigeto Nishino², Hiroshi Uchida², Hisayuki Yoshikawa³

¹ Meteorological Research Institute, ² JAMSTEC, ³ Hokkaido University

1. Abstract

In September 2013, surface seawater in the Chukchi sea and the Canada Basin had low salinity and relatively high partial pressure of CO₂ (pCO₂ > 350 μatm) compared with their in the adjacent area. This high pCO₂ was attributable to low biological activities in surface water. Despite that there was low pCO₂ (< 200 μatm) water by primary production in subsurface layer. This high pCO₂ water was likely to be affected by melt water from adjacent sea ice. In this region, nutrients in surface layer were almost depleted due to massive primary production in early summer. However, melt water which has high pCO₂ capped the subsurface layer and hampered oceanic CO₂ absorption. In the context of the long-term decline of sea ice, an inhibition of oceanic CO₂ absorption by melt water was notable phenomenon in the open Arctic Ocean.

2. Method

MR13-06 cruise of R/V *Mirai* was conducted in the Western Arctic Ocean August 28th to October 6th in 2013. Surface seawater was pumped continuously from the seachest and introduced into the shower type equilibrator for the measurement of partial pressure of CO₂ (pCO₂) and methane (pCH₄). A wavelength-scanned cavity ring-down spectrometer (Picarro, G2301) was used as a detector for CO₂ and CH₄. Temperature and salinity of pumped water were measured simultaneously. At hydrographic stations, seawater column profile for temperature, salinity and dissolved oxygen was obtained with CTD-carousel sampler equipped with sensors for dissolved oxygen. Apparent oxygen utilization (AOU) is defined as the difference between the concentration of dissolved oxygen and that of oxygen saturation calculated by Garcia and Gordon [1992]. Sample for dissolved inorganic carbon (DIC) and total alkalinity (TA) were taken along with CTD measurement. Measurements of DIC were made with total CO₂ measuring system (Nippon Ans.) based on CO₂ extraction and coulometric titration. Measurements of TA were made using a spectrophotometric technique based on single-point detection. The value of pCO₂ was calculated (pCO_{2calc}) for each discrete sample from DIC, TA, temperature and salinity. Dissociation constants of carbonic acid given by Lueker et al [2000] were used for calculation. Daily sea ice concentration was obtained by NOAA Advanced Very High Resolution Radiometer (AVHRR) and used to evaluate the extent of sea ice. We also used the net primary production Standard Products based on the Vertically Generalized Production Model by Behrenfeld and Falkowski [1997].

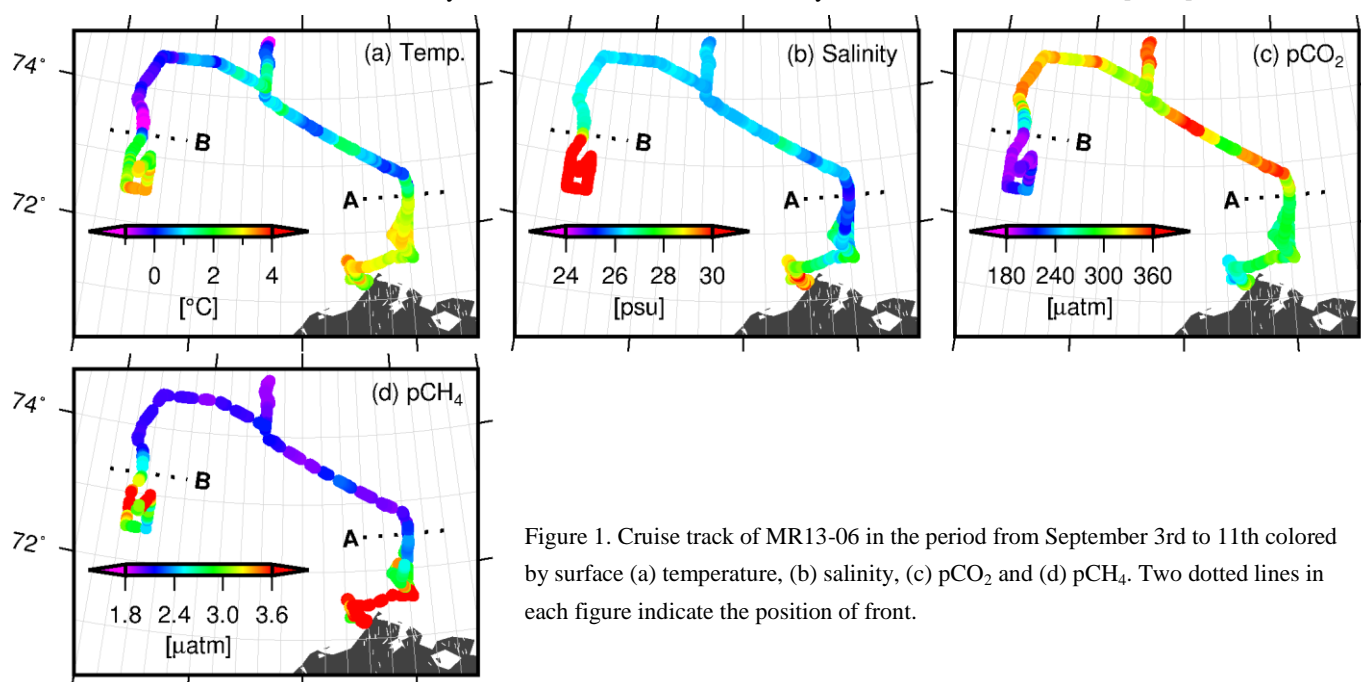


Figure 1. Cruise track of MR13-06 in the period from September 3rd to 11th colored by surface (a) temperature, (b) salinity, (c) pCO₂ and (d) pCH₄. Two dotted lines in each figure indicate the position of front.

3. Result & Discussion

According to the distribution of sea surface temperature, salinity, $p\text{CO}_2$ and $p\text{CH}_4$ along the cruise track in MR13-06 (Figure 1) there were two fronts. The one (Front A in Figure 1) was located at around 72.5°N 155°W . The other (Front B in Figure 1) was located at around 73.5°N 168°W . Large gap in $p\text{CO}_2$ was seen across the front B. To the south of the front B, low $p\text{CO}_2$ (< 200 μatm) and saline water was prevailing. However, $p\text{CO}_2$ was higher (~ 350 μatm) to the north of the front B than to the south.

CTD profiles were obtained at three stations (station 28, 34, and 38) divided by these fronts (Figure 2). Warmer and fresher surface water was seen above halocline around 20 m depth at station 28 located to the south of the front A near the Point Barrow. Shallow halocline was also seen at the station 34 although surface water was colder than that at station 28. At station 38 located at to the south of the front B, stratification and upper halocline were much weaker than the other 2 stations in station. Negative AOU layer was commonly observed at below the halocline among all 3 stations. According to the satellite image and salinity in the negative AOU layer, these oxygen supersaturation was attributable to the net primary production in the Chukushi Sea. In contrast, there were large variations in $p\text{CO}_{2\text{calc}}$ above halocline.

Satellite sea ice measurements indicated that a significant concentrations of sea ice had existed around station 34 until 2 weeks before and had disappeared by the time of observation. Fresh and cold surface water in station 34 was most likely to be affected by melt water. The strong influence of melt water was confirmed by the high salinity-normalized TA at station 34. Melt water has low density because of its low salinity, and thereby caps Chukuchi summer water. In late summer, nutrients such as nitrates and phosphate had almost depleted by the massive primary production in the Chukuchi sea. Additionally, melt water contained little nutrients. As a result, further biological activities hardly occurred in melt water. Due to the absence of biological drawdown of CO_2 , surface $p\text{CO}_2$ at station 34 was higher than station 38. Surface water at station 28 also had low salinity and density. But it had higher temperature than station 34. High surface $p\text{CH}_4$ at station 28 indicated the significant influence of riverine discharge and/or coastal upwelling. Riverine and coastal water was significantly affected by biological activities in shallow shelf region. These are the reason why $p\text{CO}_2$ at station 28 was not as high as station 34.

Melt water has a large impact on air-sea CO_2 flux. As shown in Figure 1 (c), $\Delta p\text{CO}_2$ ($= p\text{CO}_{2\text{sea}} - p\text{CO}_{2\text{air}}$; $p\text{CO}_{2\text{air}} \approx 390$ μatm) around station 38 was as large as -200 μatm . In contrast, $\Delta p\text{CO}_2$ in the region where seawater was affected by melt water was only -50 μatm . Air-sea CO_2 flux in melt water affected area was reduced to about a quarter relative to other area under the assumption that the other conditions such as temperature and wind speed were the same. Our study indicated that depending on the timing and/or location, melt water hampers the decrease in $p\text{CO}_2$ and inhibits oceanic uptake of CO_2 by capping the biologically active layer in subsurface.

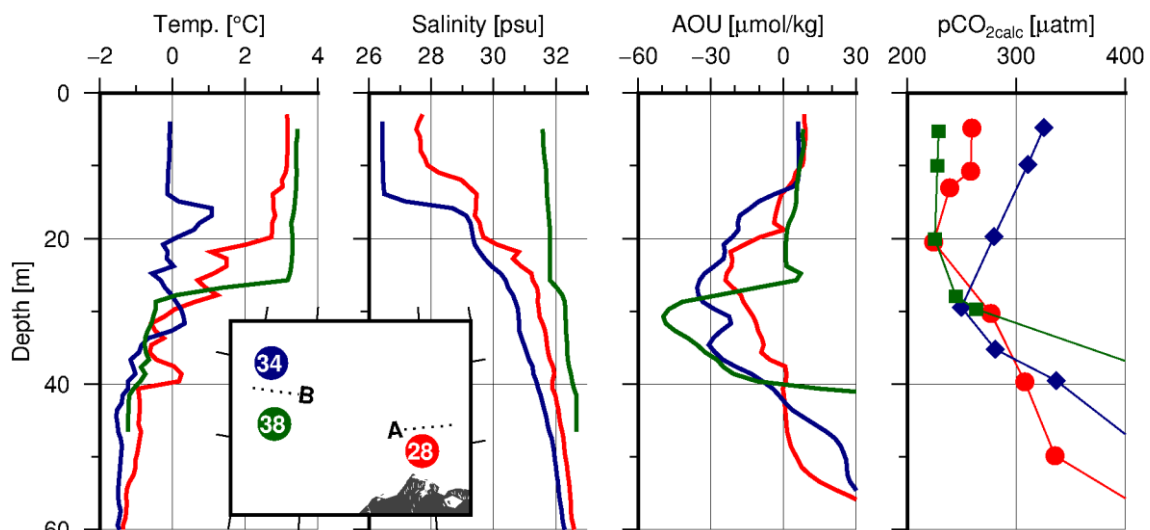


Figure 2 Column profiles of temperature, salinity, AOU, and $p\text{CO}_{2\text{calc}}$ in MR13-06. Red, blue and green lines indicate the profiles at station 28, 34 and 38, respectively, shown in the map.

References

- Behrenfeld, M. J., and P. G. Falkowski (1997), Photo synthetic rates derived from satellite-based chlorophyll concentration, *Limnol. Oceanogr.*, **42**, 1-20.
- Garcia and Gordon (1992), Oxygen solubility in seawater; Better fitting equations. *Limnol. Oceanogr.* **37**(6), 1307-1312.
- Lueker, T.J., A.G. Dickson, and C.D. Keeling, (2000), Ocean $p\text{CO}_2$ calculated from dissolved inorganic carbon, alkalinity, and equations for K_1 and K_2 : Validation based on laboratory measurements of CO_2 in gas and seawater at equilibrium. *Marine Chemistry*, **70**, 105–119.